“© 2017 IEEE. Personal use of this material is permitted. Permission from IEEE must be obtained for all other uses, in any current or future media, including reprinting/republishing this material for advertising or promotional purposes, creating new collective works, for resale or redistribution to servers or lists, or reuse of any copyrighted component of this work in other works.”

Design of a Lock-in Amplifier Integrated with a Coil System for Eddy-Current Non-Destructive Inspection

Fredy Munoz, Jaime Valls Miro, Gamini Dissanayake, Nalika Ulapane, Linh Nguyen

University of Technology Sydney, Australia

Emails: Fredy.Munoz@uts.edu.au, Jaime.VallsMiro@uts.edu.au, Gamini.Dissanayake@uts.edu.au, Nalika.Ulapane@uts.edu.au,VanLinh.Nguyen@uts.edu.au

***Abstract*—Eddy-current non-destructive inspections of conductive components are of great interest in several industries including civil infrastructure and the mining industry. In this work, we have used a driver-pickup coil system as the probe to carry out inspection of ferromagnetic plates. The specific geometric configuration of the probe generates weak electric signals that are buried in a noisy environment. In order to detect these weak signals, we have designed and implemented a lock-in amplifier as part of the signal processing technique to increase the signal-to-noise ratio and also improve the sensitivity of the probe. We have used Comsol as a finite element method (FEM) to design the probe and conducted experiments with the probe and the lock-in amplifier. The experimental results, which are in agreement with the FEM results, indicate that the designed probe along with a lock-in amplifier can potentially be used to estimate the thickness of thin plates while reducing the effects of the liftoff on the measurements.**

I. Introduction

The detection of defects such as cracks in critical metal structures and the assessment of the condition of metallic water mains are commonly performed by using Eddy-current non-destructive inspection (NDI) [1-7]. In this technique, a coil excited with alternating current, called driver coil, is placed above the metal component in which eddy currents are induced. A second coil, called pickup coil, is also placed above the component to measure changes in the voltage across the pickup coil. These changes in the voltage carry information about the defects and the thickness of the metal component.

Different geometrical configurations, coil shapes and orientations are possible with a driver-pickup coil system. For instance, the analysis of six different high-symmetry configurations, including the pancake coil geometry, for cylindrical coils is presented in [8]. Although the analysis and implementation of driver-pickup coil systems have been extensively reported to work on homogeneous metal components such as steel, limited work has been reported on ferromagnetic components such as cast iron which can be highly heterogeneous [9]. In this work, we focus on the condition assessment of cast iron components by using Eddy-current NDI. Specifically, we aim to estimate the thickness of cast iron components from the voltage measured across a pickup coil.

A probe consisting of a driver-pickup coil system arranged in a pancake geometry is the most widely used in practice and is the probe that we have adopted in this work. In this configuration for air-cored cylindrical coils, we exploit the separation distance to improve the sensitivity of the probe while reducing the effect of the coil liftoff. However, as the separation of the coils is increased, the voltage received at the pickup coil becomes weaker and the signal-to-noise ratio (SNR) deteriorates.

In order to improve the SNR and the sensitivity of the probe to changes in the thickness of the cast iron component, we propose the use of a lock-in amplifier. Other signal processing techniques, such as homomorphic filter and pulse compression, have been reported in the literature to improve the SNR and enhance the detection reliability [10-11]. However, these techniques are usually more complex than lock-in amplifiers. Therefore, the main objective of this work is to determine whether a lock-in amplifier is sufficient to improve the SNR and the sensitivity of the specific probe that we have designed to conduct NDI.

The remainder work is organized as follows. Section II provides a description of the driver-pickup coil system that is used as a probe to measure the thickness of cast iron components. The details of the lock-in amplifier, as a signal processing technique, are presented in Section III. Experimental results of the probe and the lock-in amplifier are presented in Section IV. Finally, the significance of the results and future work are discussed in Section V.

II. The Driver-Pickup Coil System

The driver-pickup coil system consists of a pair of cylindrical air-cored coils that are placed above a cast iron plate as shown in Fig. 1. The plate is large enough so that edge effects are minimized. In this work, we focus on metallic plates that have a non-ferromagnetic insulation layer of 10 mm in thickness.

The driver coil has 300 turns, a_{1d}: 25 mm, a_{2d}: 31 mm, height (h_{2d}-h_{1d}): 10 mm, wire diameter: 0.2 mm, and is excited with 10 V at 10 Hz. The pickup coil has 200 turns, a_{1p}: 14 mm, a_{2p}: 22 mm, height (h_{2p}-h_{1p}): 5 mm, wire diameter of 0.2 mm. The distance d between the centre of the coils is changed to improve

the sensitivity of the probe and reduce the effect of the liftoff on the measurements. The liftoff of the two coils is the same (i.e., h_{1d}= h_{1p}) and can vary from 10 mm to 20 mm. The total voltage across the pickup coil can be described as $V_r(t)=V_s(t)+n(t)$, where $V_s(t)$ represents the signal that varies with the liftoff and thickness of the inspected plate and n(t) represents electrical noise in the system.

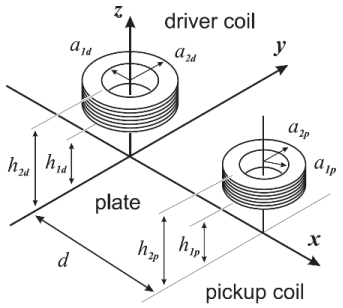

Fig. 1. Pair of air-cored coils forming a driver-pickup system above a cast iron plate with a thickness c protected by a 10 mm thick insulation layer

We are interested in measuring the amplitude, A, and phase, ∅, of the voltage V_s as the liftoff and thickness of the plate, c, vary. For this reason, we built a lock-in amplifier that allows us to measure $V_s=A\sin(\omega t+\emptyset)$ in steady state that is buried in a noisy environment (i.e., n(t)) and the experimental results are presented in Section IV. Prior to the experimental results, we have also used a FEM solution (Comsol Multiphysics) for a quick design and prototype of the probe and the results are presented as follows.

We have used a 2D axisymmetric model with the driver coil's axial axis coinciding with the Z axis and the bottom of its rectangular cross section (i.e., the liftoff) varies from 10 to 20 mm (see Fig. 2). The conducting plate is simulated with a large disk-shaped cast iron plate the thickness of which can vary from 3 mm to 15 mm. The driver coil is simulated with copper (electrical conductivity σ = 5.9e7 S/m and magnetic permeability u_r =1) and the conducting plate with cast iron (electrical conductivity σ = 2.7e6 S/m and magnetic permeability u_r=60). We only simulate the driver coil in a 2D axisymmetric model because this model provides sufficient results to achieve our goals in this paper. However, both coils can be also simulated in a 3D model to improve accuracy in the results at the expense of longer computational time.

We estimate changes in the amplitude of B_z along the line L due to changes in the liftoff and the thickness c of the conducting plate. Therefore, the line L represents the separation distance d between the two coils and the system is simulated assuming steady state (thus we use a frequency domain analysis in our simulations). The approximate magnitude of V_s can be obtained from B_z which is generated by the driver coil. The results of the amplitude of B_z as a function of d for three different liftoffs and for three different plate's thicknesses are shown in Fig. 3 a) and b), respectively. In these FEM results, the amplitude of B_z is computed as follows:

$$|B_z| = \sqrt{\text{real}(B_z)^2 + \text{imag}(B_z)^2} \quad (1)$$

and the approximate amplitude of V_s can be computed as

$$|V_s| = NA_i\omega|B_z| \quad (2)$$

where N represents the number of turns of the pickup coil, A_i represents the area created by the inner loop of the pickup coil (i.e., $A_i=\pi(a_{1p})^2$) and ω is the angular frequency, in rad/s, at which the driver coil is excited (i.e., $\omega=2\pi f$).

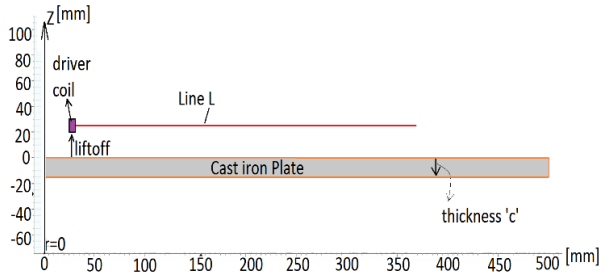

Fig. 2 2D Axisymmetric model used in Comsol

According to these results for B_z, the amplitude of B_z is sensitive to the liftoff for 50 mm<d<200 mm and its sensitivity to the liftoff, $\frac{\Delta B_z}{\Delta liftoff}$, decreases for d>200 mm (and $\frac{\Delta V_s}{\Delta liftoff}$ also decreases for d>200 mm). On the contrary, the sensitivity of the amplitude of B_z to changes in the plate's thickness, $\frac{\Delta B_z}{\Delta c}$, increases for d>200 mm (and $\frac{\Delta V_s}{\Delta c}$ also increases for d>200 mm). Ideally, the probe should have $\frac{\Delta B_z}{\Delta c}>>\frac{\Delta B_z}{\Delta liftoff}$ (or $\frac{\Delta V_s}{\Delta c}>>\frac{\Delta V_s}{\Delta liftoff}$), consequently the pickup coil should be located at a distance d>200 mm. For example, at d=200 mm, $|B_z| \cong 7$ uT (see Fig. 3) and using (2) we can estimate $|V_s|$ <300 uV. However, the amplitude of B_z decreases as d is further increased as shown in Fig. 3. Since V_s is linearly dependent on $|B_z|$ as indicated in (2), then the voltage V_s is expected to be small (smaller than 300 uV for d>200 mm) and buried in a noisy environment. These are the main reasons why we have implemented a lock-in amplifier to recover V_s. The details of the lock-in amplifier are presented in the following section (Section III).

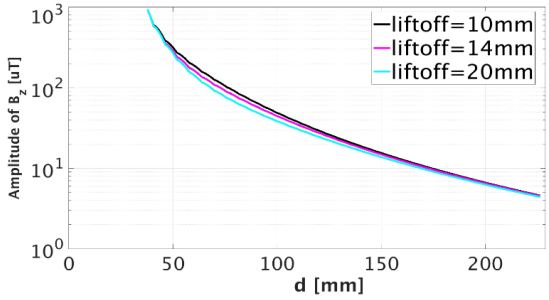

(a)

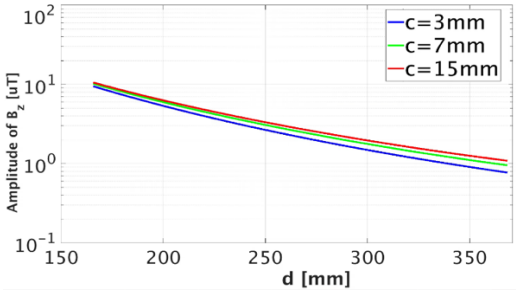

(b)

Fig. 3 Amplitude of B_z as a function of d for three different: a) liftoffs (plate's thickness is 13 mm), b) thicknesses (liftoff is 20 mm)

III. THE LOCK-IN AMPLIFIER

The block diagram of the implemented dual-phase lock-in amplifier is shown in Fig. 4. The input of the lock-in amplifier is $V_r(t)$, and the two DC outputs are X and Y. The signal received in the pickup coil, $V_r(t)$, is amplified by a factor K before being demodulated. The final stage consists of two low-pass filters (LPFs) that can be used to obtain the DC components X and Y from which we can estimate the amplitude of $V_s(t)$ and its phase (i.e., A and $\emptyset$).

In order to single out V_s from the noise n(t), we need to provide a reference signal $V_{ref}(t)$ that shares the same frequency with V_s. We can select for example a reference signal given by

$$V_{ref}(t) = \sin(\omega t). \quad (3)$$

Assuming that n(t) can be represented as a linear combination of sinusoidal waves, then we can approximate the amplified voltage in the pickup coil as

$$V_r(t) = AK\sin(\omega t + \emptyset) + \sum_{i=0}^{\infty} B_i K \sin(\omega_i t + \theta_i). \quad (4)$$

By multiplying (3) and (4), we obtain the output of the first demodulator as

$$V_{d1}(t) = \frac{AK}{2}[\cos(\emptyset) - \cos(2\omega t + \emptyset) + \sum_{i=0}^{\infty} \frac{B_i K}{2}[\cos((\omega_i - \omega)t + \theta_i) - \cos((\omega_i + \omega)t + \theta_i)] \quad (5)$$

Due to the randomness of the noise, we can assume that in general $\omega_i \neq \omega$, and if we suppress the high frequencies of V_{d1} by using a LPF, the output X of the first LPF can be approximated as

$$X = \frac{AK}{2}\cos(\emptyset) \quad (6)$$

Similarly, if $V_{ref}(t) = \cos(\omega t)$ and we multiply it by (4), we obtain the output of the second demodulator as

$$V_{d2}(t) = \frac{AK}{2}[\sin(\emptyset) - \sin(2\omega t + \emptyset) + \sum_{i=0}^{\infty} \frac{B_i K}{2}[\sin((\omega_i - \omega)t + \theta_i) - \sin((\omega_i + \omega)t + \theta_i)] \quad (7)$$

And if we use a second LPF to suppress the high frequencies of V_{d2}, the output Y of the second LPF can be approximated as

$$Y = \frac{AK}{2}\sin(\emptyset) \quad (8)$$

Finally, A and $\emptyset$ can be estimated from (6) and (8) as follows:

$$A = \frac{2}{K}\sqrt{X^2 + Y^2} \quad (9)$$

$$\emptyset = \tan^{-1}\left(\frac{Y}{X}\right). \quad (10)$$

Since the frequency of operation of the coils is 10 Hz, it is difficult with analog LPFs to obtain a clear DC output. According to (5) and (7), ripple signals with a frequency of 2ω will be mixed with the DC outputs and the amplitude of the ripple will depend on the roll-off of the LPF. Besides the problem of the ripple signals, the analog LPF will have a slow response to changes in the signal because the cutoff frequency f_c is small (i.e., the time constant of the lock-in amplifier $\tau = \frac{1}{2\pi f_c}$ is long).

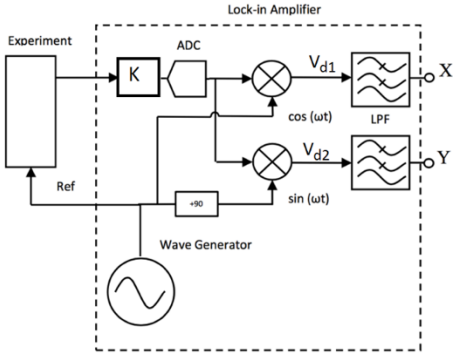

Fig. 4. Digital dual-phase lock-in amplifier. V_{d1} and V_{d2} represent the outputs of the demodulators

To overcome the issue of the ripple generated when using first-order LPFs, we could use higher-order LPFs to improve the roll-off and thus minimize the amplitude of the ripple signal. However, this approach would increase the complexity of the system and the system would still respond very slowly before the DC signal stabilizes as τ is determined by f_c.

The importance of the ripple and the response time τ depends on the particular application. In our application, minimizing the amplitude of the ripple is the most important factor to obtain greater accuracy and sensitivity to changes in the liftoff and thickness of the plate. Therefore, we have decided to demodulate $V_r(t)$ and also implement the LPFs in software. To this end, we firstly compute the fast Fourier transform (FFT) of $V_{d1}(t)$ and $V_{d2}(t)$: $V_{d1}(f)$ and $V_{d2}(f)$, respectively. Secondly, we extract their DC components which correspond to the amplitudes at f=0 Hz (i.e., $2*|X| = |V_{d1}(f=0)|$ and $2*|Y| = |V_{d2}(f=0)|$). Finally, we use (9) and (10) to estimate the amplitude and phase of $V_s(t)$. Besides the software implementation, we have implemented in hardware the amplification stage which consists of two op-amps in cascade to adjust the gain K and the details of the experimental setup are described in the next section (Section IV).

IV. EXPERIMENTAL RESULTS

We fabricated the driver-pick up coil system with the parameters described in Section II. The two bobbins were fabricated in a 3D printer and mounted on 3 different plastic platforms (each platform with a fix d) as shown in Fig. 5. In our experiments, we varied the liftoff, the separation distance d and the frequency of the driver coil. Three pairs of small plastic blocks with heights of 10, 15 and 20 mm were placed under the coils to adjust the liftoff of the probe. We carried out our experiments on a 12 mm thick cast iron plate with an area of 600x1500 mm^2. The coils were placed in the centre of the plate to minimize the edge effects on the measurements.

A two-stage cascaded circuit with op-amps was used to amplify $V_r(t)$. The first stage consisted of a differential amplifier (AD620) and the second stage was used as a non-

inverting amplifier (OP27). The driver coil was excited with a sinusoidal wave of 120 mV generated in a PC that was amplified 100 times with a non-inverting amplifier (OPA548). A data acquisition unit (DAQ, NI USB-6221) was used to collect the data from the pickup coil and also to excite the driver coil.

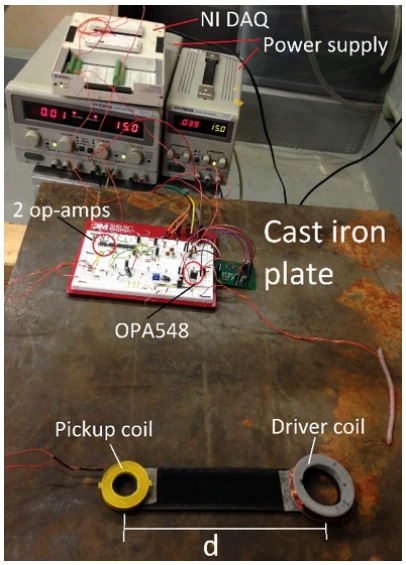

Fig. 5. Experimental setup. The platform in this figure that holds the coils has a separation distance of d=195 mm. Two other plastic platforms were used with d=260 and 340 mm

In the first set of experiments, we aimed to characterize the noise in the system. To this end, we connected the pickup coil to the output of the differential amplifier which was set with a gain of 1. The coils were tested in the air at a distance d of 340 mm and the driver coil was excited at 10 Hz. The voltage across the pickup coil in the time and frequency domains is shown in Fig. 6. The maximum amplitude of V_r was estimated to be approximately 39 mV at 10 Hz and the amplitudes of the rest of harmonics were less than 10 mV as shown in Fig. 6 b). We repeated this experiment for d=180, 260 and 340 mm and for 5 different frequencies. We always obtained the highest amplitudes at the same frequencies of the excitation signal and the amplitudes of the harmonics were always smaller. The results of these experiments are shown in Fig. 7 which only shows the maximum amplitudes of V_r.

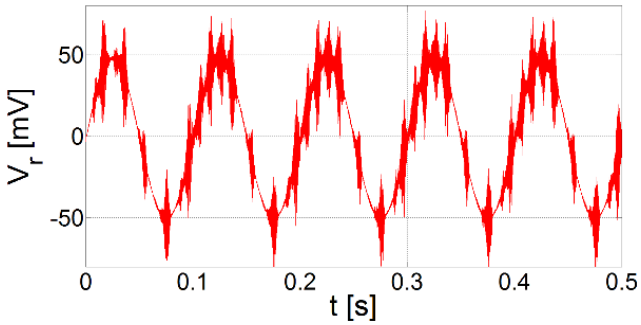

(a)

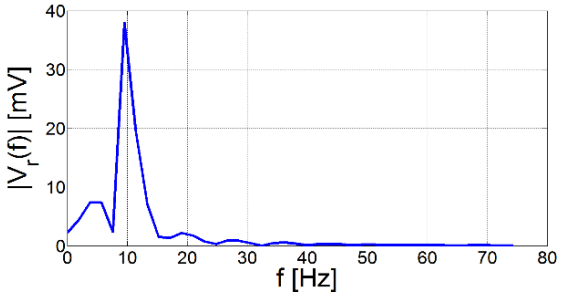

(b)

Fig. 6. Vr(t): a) time domain, b) frequency domain (computed by using the FFT)

According to the results shown in Fig. 7, $|V_r| \cong 39$ mV for any d and f such 180 mm<d<340 mm and 10 Hz<f<50 Hz. Considering that $|V_s|$<300 uV when d>200 mm at 10 Hz (as presented in Section II), we conclude that the voltage across the pickup coil V_r is mainly due to noise. Therefore, V_s is buried in noise n(t) that has an amplitude of approximately 39 mV at the same frequency of the excitation signal and its harmonics have smaller amplitudes.

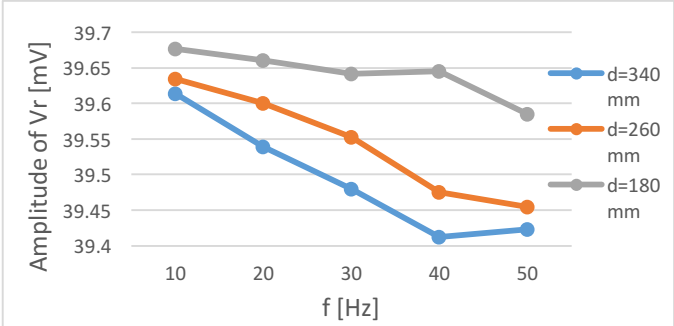

Fig. 7. Amplitude of V_r estimated at the same frequency of excitation. V_r is predominantly noise induced at the pickup coil

Since the amplitude of the noise at 10 Hz was estimated to be approximately 39 mV, then the magnitude of V_s should be larger than 40 mV to reduce the influence of the noise at the output of the lock-in amplifier and to enhance the sensitivity of the system. For these two reasons, in our second set of experiments, we put the two coils with a separation distance of 340 mm in the air and set up the AD620 with a gain of 1000 and the OP27 with a gain of 100. With these gains, the amplitude of the amplified V_s would be greater than 2 V but smaller than 10 V to avoid the saturation of the op-amps. The output of V_r after being amplified by approximately 1.08e5 times is shown in Fig. 8.

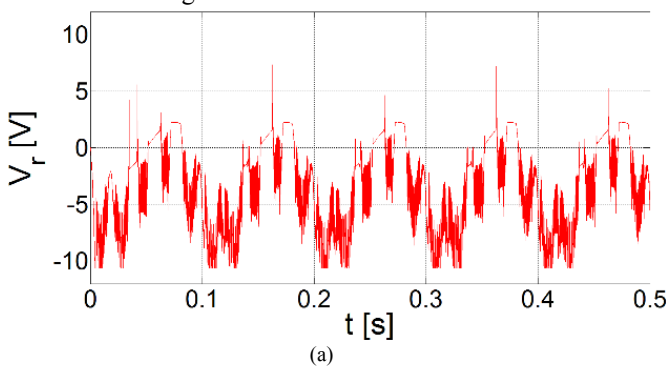

(a)

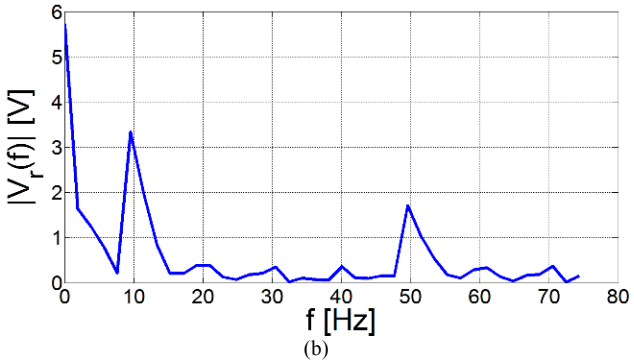

(b)

Fig. 8. Vr(t) amplified by 1.08e5 times: a) time domain, b) frequency domain

In Fig. 8 a), the first 100 ms differs from the other four cycles of V_r due to a transient response. Therefore, only the last four cycles of V_r were considered to compute the FFT and the amplitude of V_r in the frequency domain is shown in Fig. 8 b).

This V_r was passed through the lock-in amplifier which estimated an output of 3.4 V (i.e., $3.4=2\sqrt{X^2+Y^2}$). By using (9), and subtracting the amplitude of the noise of 39 mV, we have estimated an amplitude A= 31 uV (31 uV=(3.4-0.039)/ *1.08e5). Thus, the lock-in amplifier is able to pick up $|V_s|$= 31 uV even when there is noise of 39 mV at the same frequency. This represents an improvement in the SNR of at least 30 db.

In the final set of experiments, we tested the pair of coils above a cast iron plate with a constant thickness of 12 mm and only varied the liftoff and the distance d. The aim of these final experiments is to validate if the sensitivity of V_s to the liftoff, $\frac{\Delta V_s}{\Delta liftoff}$, decreases as discussed in Section II. In the first experiment, we placed the coils at d=340 mm, liftoff=10 mm and excited the driver coil at 10 Hz. The total gain with the two op-amps was set to K=24390 (differential amplifier with a gain of 1074) to obtain an amplified V_r in the range between 1 V and 10 V. Fig. 9 shows the output of the demodulators in the frequency domain.

We obtained: 2*X=-0.255*2=-0.51 V ($|V_{d1}(f=0)|$=0.51 V as shown in Fig. 9 a)), 2*Y=-0.85*2=-1.7 ($|V_{d2}(f=0)|$=1.7 V as shown in Fig. 9 b)), $2*\sqrt{X^2+Y^2}$ =1.77 V. Thus, the amplitude of V_s is A= 71.1 uV ((1.77-0.039)/K). We repeated this experiment for three different liftoffs (10, 15 and 20 mm), carrying out eight experiments for each liftoff, and for three different separation distances (195, 260 and 340 mm). Thus, a total of 72 experiments were conducted. The total gain K was adjusted to 11802 for d=195 and 260 mm to make sure that the amplified signal V_r was larger than 1 V but smaller than 10 V. Fig. 10 a) and b) show the output of the lock-in amplifier (i.e., $2*\sqrt{X^2+Y^2}$) for d=260 mm and d=340 mm, respectively. We also averaged the output of the lock-in amplifier and subtracted the noise (the 39 mV) from it to estimate the amplitude of V_s. These results are summarized in Table I.

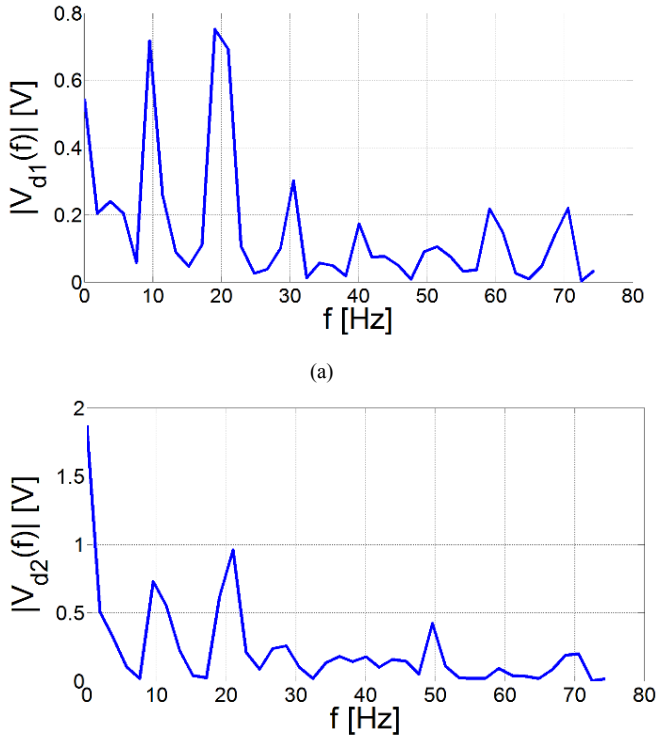

(a)

(b)

Fig. 9. Output of demodulators in the frequency domain. The gain of the op-amps was set up to K=24390

According to the experimental results in Table I, $\frac{\Delta V_s}{\Delta liftoff}$=4.7 uV/mm for d=195 mm, and $\frac{\Delta V_s}{\Delta liftoff}$ decreases to 0.45 uV/mm for d=340 mm. These experimental results are in agreement with those obtained from Comsol which are presented in Section II and indicate that the probe would be less sensitive to changes in the liftoff as d increases. We also expect that the probe is more sensitive to changes in the thickness of the plate as d increases (i.e., $\frac{\Delta V_s}{\Delta c}\uparrow$ as d $\uparrow$). Although $\frac{\Delta V_s}{\Delta c}$ was not experimentally measured in this work for different separation distances, it will be the focus of our future work.

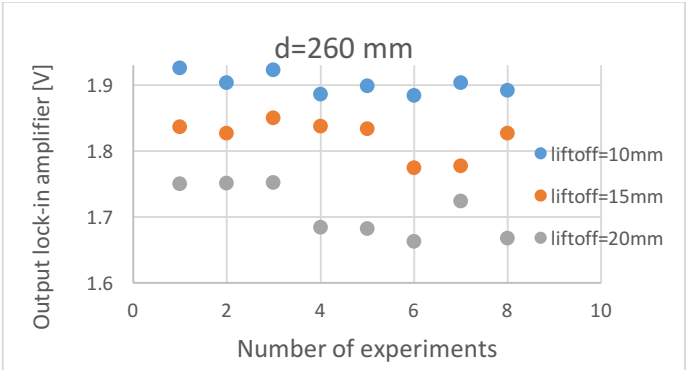

(a)

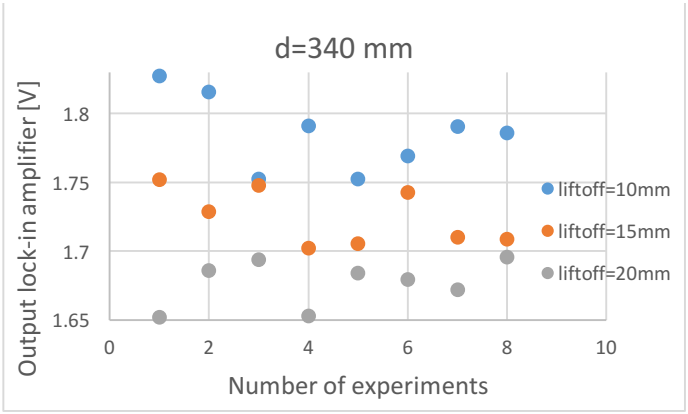

(b)

Fig. 10. Output of the lock-in amplifier for: a) d=260 mm, b) d=340 mm

Table I. Amplitude of $V_s(t)$ in uV

liftoff [mm]	d=195 [mm]	d=260 [mm]	d=340 [mm]
10	349.5	157.8	71.6
15	304.8	150.9	69.1
20	302.8	141.5	67.1

V. Conclusions and Future Work

We have presented in this work a lock-in amplifier as part of a signal processing technique that is to operate with a probe to perform non-destructive inspections. We have shown that the lock-in amplifier is able to recover small signals generated in a pickup coil that can be buried in a noisy environment. Specifically, we have found that a signal with an amplitude of 31 uV can be recovered even when the noise is 1000 times larger at the same frequency of operation. This improvement in the SNR obtained by using the lock-in amplifier also provides an enhancement of the sensitivity of the probe. By tuning the lock-in amplifier through changes in the total gain of the op-amps, we were able to obtain a sensitivity of 0.45 uV/mm. The experimental results, which are in agreement with the theoretical results, indicate that a properly tuned lock-in amplifier can be potentially used to measure variations in the thickness of cast iron plates, although this work is left for our future work.

References

[1] B. A. Auld, and J. C. Moulder, "Review of Advances in Quantitative Eddy Current Nondestructive Evaluation", Journal of Nondestructive Evaluation, vol. 18, No. 1, 1999.

[2] M.Ph. Papaelias, C. Roberts, and C.L. Davis, "A review on non-destructive evaluation of rails: State-of-the-art and future development ", Proceedings of the Institution of Mechanical Engineers, Part F: Journal of Rail and Rapid Transit, vol. 222, Issue 4, pp. 367-384, 2008.

[3] C. Ye, J. Xin, Z. Su, L. Udpa, and S. S. Udpa, "Novel Transceiver Rotating Field Nondestructive Inspection Probe", IEEE Transactions on Magnetics, vol. 51, No. 7, Jul. 2015.

[4] R. Falque, T. Vidal-Calleja, J. V. Miro, D. C. Lingnau, and D. E. Russell, "Background Segmentation to Enhance Remote Field Eddy Current Signals", Australasian Conference on Robotics and Automation, Melbourne, Australia, Dec 2-4 2014.

[5] S. M. Haugland, "Fundamental Analysis of the Remote-Field Eddy-Current Effect", IEEE Transactions on Magnetics, vol. 32, No. 4, Jul. 1996.

[6] Y. S. Sun, S. Udpa, W. Lord, and D. Cooley, "Inspection of Metallic Plates Using a Novel Remote Field Eddy Current NDT Probe", Review of Progress in Quantitative Nondestructive Evaluation, vol. 15, pp. 1137-1144, 1996.

[7] Y.S. Sun, W. Lord, L. Udpa, S. Udpa, S.K. Lua, and K.H. Ng, "Thick-walled Aluminum Plate Inspection Using Remote Field Eddy Current Techniques", Review of Progress in Quantitative Nondestructive Evaluation, vol. 16, pp. 1005-1012, 1997.

[8] S. K. Burke, and M. E. Ibrahim, "Mutual impedance of air-cored coils above a conducting plate", Journal of Physics D: Appl. Phys., vol. 37, pp. 1857-1868, 2004.

[9] R. Falque, T. Vidal-Calleja, G. Dissanayake, and J. V. Miro, "From the Skin-Depth Equation to the Inverse RFEC Sensor Model", International Conference on Control, Automation, Robotics and Vision, Phuket, Thailand, Nov. 13-15, 2016.

[10] X. Xu and F. Luo, "Optimal sensor design and digital signal processing techniques for remote field eddy current testing", Insight: Non-Destructive Testing and Condition Monitoring, vol. 48, No. 7, pp. 421-425, Jul. 2006.

[11] J. Isla, and F. Cegla, "Coded Excitation for Low SNR Pulse-Echo Systems: Enabling Quasi-Real-Time Low-Power EMATs", IEEE International Ultrasonics Symposium, Tours, France, Sep. 18-21 2016.